

Supporting Information

Kinetics and Mechanism of the Co(II)-assisted Oxidation of L-Ascorbic Acid by Dioxygen and Nitrite in Aqueous Solution

Elena A. Vlasova, Natalya Hessenauer-Ilicheva, Denis S. Salnikov, Evgeny V. Kudrik,
Sergei V. Makarov and Rudi van Eldik

Legends for Figures

Figure S1: Typical kinetic traces recorded for the reaction of complex **I** with L-ascorbic acid at 510 nm. Experimental conditions: $[I] = 2 \times 10^{-5}$ M, $[H_2A]_T = 0.28$ mM, 0.1 M acetate buffer (pH 5.8, solid line) and 0.1 M TRIS buffer (pH 7.0, dashed line) at 25°C .

Figure S2: Plots of $1/k_{obs}$ vs. $1/[H_2A]_T$ as a function of temperature. Experimental conditions: $[\text{Co}^{II}(\text{L})(\text{H}_2\text{O})_2]^{8-} = 2 \times 10^{-5}$ M, $[H_2A]_T = (0.14 - 1.0)$ mM, 0.1 M acetate buffer (pH = 5.8).

Figure S3: Plot of k_{obs} vs. $[H_2A]_T$ for the reduction of complex **I** by L-ascorbic acid under anaerobic conditions. Experimental conditions: $[I] = 2 \times 10^{-5}$ M, $[H_2A]_T = (0.14 - 1.0)$ mM, 0.1 M acetate buffer (pH = 3.8) at 25°C .

Figure S4: Plot of $\ln K_4$ versus $1/T$ for the reaction of complex **I** with ascorbate. Experimental conditions: $[I] = 2 \times 10^{-5}$ M, $[H_2A]_T = (0.14 - 1.0)$ mM, 0.1 M acetate buffer (pH = 5.8).

Figure S5: Eyring plot for reaction of complex **I** with L-ascorbic acid. Experimental conditions: $[I] = 2 \times 10^{-5}$ M, $[H_2A]_T = (0.14 - 1.0)$ mM, 0.1 M acetate buffer (pH = 5.8).

Figure S6: Plot of $\ln k_{obs}$ vs. pressure for the reaction between complex **I** and L-ascorbic acid. Experimental conditions: $[I] = 2 \times 10^{-5}$ M, $[H_2A]_T = 0.14$ mM, 0.1 M MES buffer (pH = 5.8) at 25°C .

Figure S7: Plot of $\ln K$ versus $1/T$ for the reaction of complex **I** with ascorbate. Experimental conditions: $[I] = 2 \times 10^{-5}$ M, $[H_2A]_T = (0.14 - 1.0)$ mM, 0.1 M TRIS buffer (pH = 7.1).

Figure S8: Eyring plot for the reaction of complex **I** with ascorbate. Experimental conditions: $[I] = 2 \times 10^{-5}$ M, $[H_2A]_T = (0.14 - 1.0)$ mM, 0.1 M TRIS buffer (pH = 7.1).

Figure S9: ESR spectrum of the product of the reaction between **I** and L-ascorbic acid under anaerobic conditions. Experimental conditions: $[I] = 2.5 \text{ mM}$, $[H_2A]_T = 62.5 \text{ mM}$, $0.3 \text{ M TRIS buffer (pH = 7.4)}$ at 85 K . The spectrum clearly shows the presence of Co^{II} at 2660 G (see J. Krzystek, A. Ozarowski, J. Telser, *Coord. Chem. Rev.*, 2006, **250**, 2308) and L-ascorbic acid signals between 2750 and 3000 G (see J. T. Masiakowski and A. Lund, *J. Chem. Soc., Faraday Trans.*, 1987, **83**, 1869). The spectrum was recorded using the following parameters: number of scans = 4, center of field = 3000 G , sweep width = 2500 G , resolution = 8192 points, microwave frequency = 8.9 GHz , microwave power = 1 mW , modulation frequency = 100 kHz , modulation amplitude = 2 G , time constant = 100 ms , and sweep time = 120 s .

Figure S10: Dependence of the induction period on $[H_2A]_T$. Experimental conditions: $[I^{\text{red}}] = 2 \times 10^{-5} \text{ M}$, $[O_2] = 0.2 \text{ mM}$, $[H_2A]_T = (0.035 - 0.14) \text{ mM}$, $0.1 \text{ M TRIS buffer (pH = 7.0)}$ at $25 \text{ }^\circ\text{C}$.

Figure S11: Eyring plot for the oxidation of reduced complex **I** by O_2 . Experimental conditions: $[I^{\text{red}}] = 2 \times 10^{-5} \text{ M}$, $[O_2] = 0.6 \text{ mM}$, $[H_2A]_T = 0.035 \text{ mM}$, $0.1 \text{ M TRIS buffer (pH = 7.0)}$.

Figure S12: Plot of $\ln k_{obs2}$ vs. pressure for the oxidation of the reduced form of complex **I** by O_2 . Experimental conditions: $[I^{\text{red}}] = 2 \times 10^{-5} \text{ M}$, $[O_2] = 0.6 \text{ mM}$, $[H_2A]_T = 0.035 \text{ mM}$, $0.1 \text{ M TRIS buffer (pH = 7.0)}$ at $35 \text{ }^\circ\text{C}$.

Figure S13: Spectral changes observed during the oxidation of the reduced form of complex **I** by nitrite. Experimental conditions: $[I^{\text{red}}] = 2 \times 10^{-5} \text{ M}$, $[H_2A]_T = 0.07 \text{ mM}$, $[NaNO_2] = 100 \text{ mM}$, $0.1 \text{ M TRIS buffer (pH = 7.0)}$ at $25 \text{ }^\circ\text{C}$. Induction period omitted for clarity.

Figure S14: Eyring plot for the oxidation of the reduced form of complex **I** by $NaNO_2$. Experimental conditions: $[I^{\text{red}}] = 2 \times 10^{-5} \text{ M}$, $[H_2A]_T = 0.14 \text{ mM}$, $[NaNO_2] = 100 \text{ mM}$, $0.1 \text{ M TRIS buffer (pH = 7.0)}$.

Figure S15: Plot of $\ln k_{obs3}$ vs. pressure for the oxidation of the reduced form of complex **I** by $NaNO_2$. Experimental conditions: $[I^{\text{red}}] = 2 \times 10^{-5} \text{ M}$, $[H_2A]_T = 0.14 \text{ mM}$, $[NaNO_2] = 80 \text{ mM}$, $0.1 \text{ M TRIS buffer (pH = 7.0)}$ at $35 \text{ }^\circ\text{C}$.

Figure S16: ^{15}N NMR spectrum recorded following the catalyzed oxidation of L-ascorbic acid by $Na^{15}\text{NO}_2$. Experimental conditions: $[I^{\text{red}}] = 2 \text{ mM}$, $[H_2A]_T = 0.14 \text{ mM}$, $[NaNO_2] = 2 \text{ M}$, $99\% D_2O$ at $25 \text{ }^\circ\text{C}$.

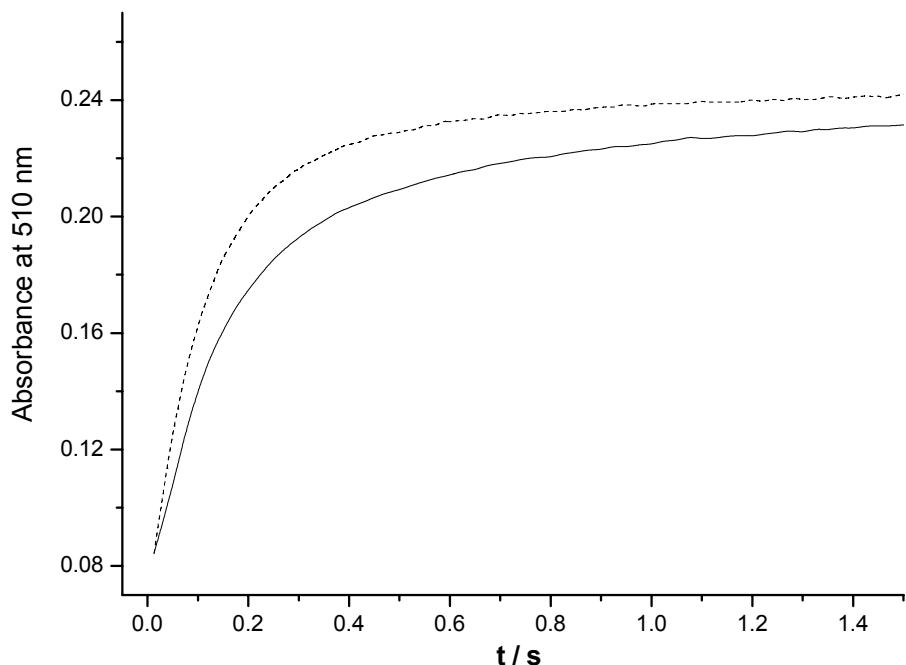


Figure S1

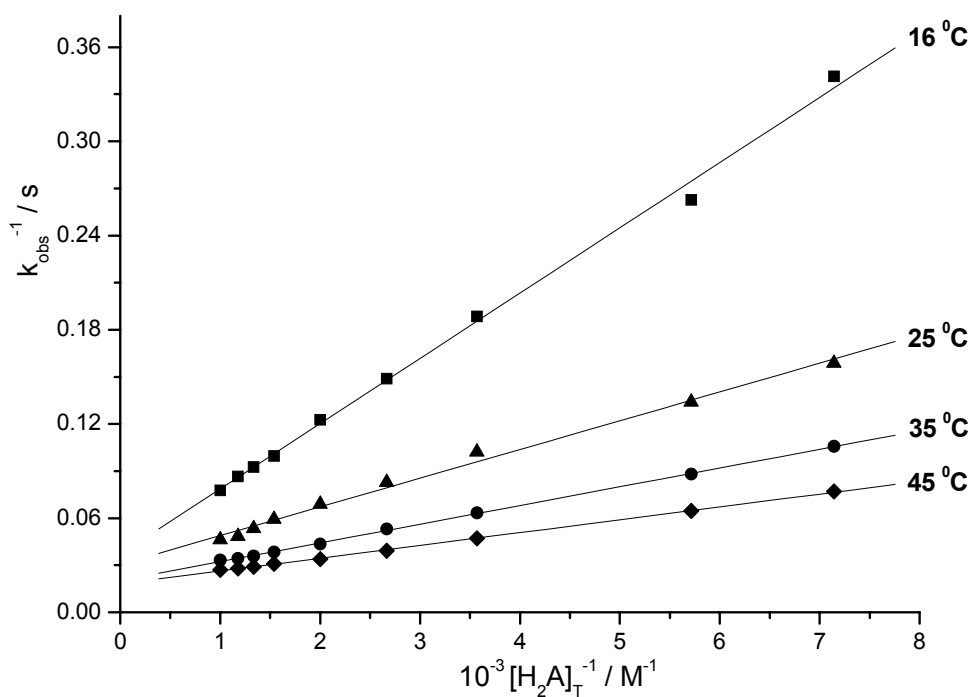


Figure S2

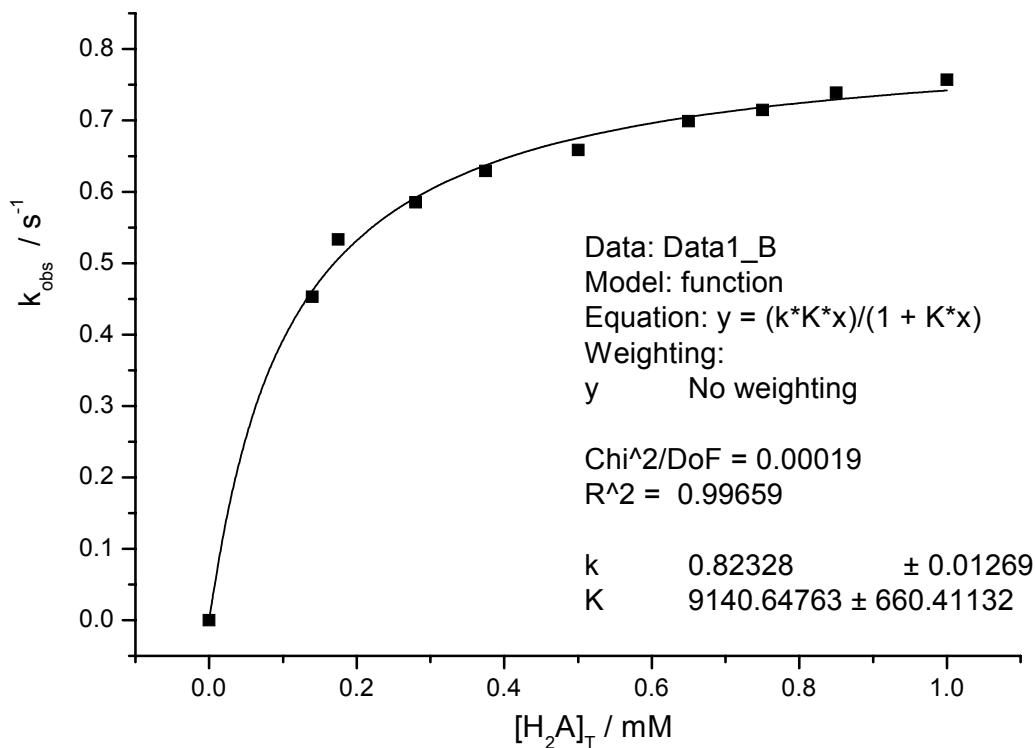


Figure S3

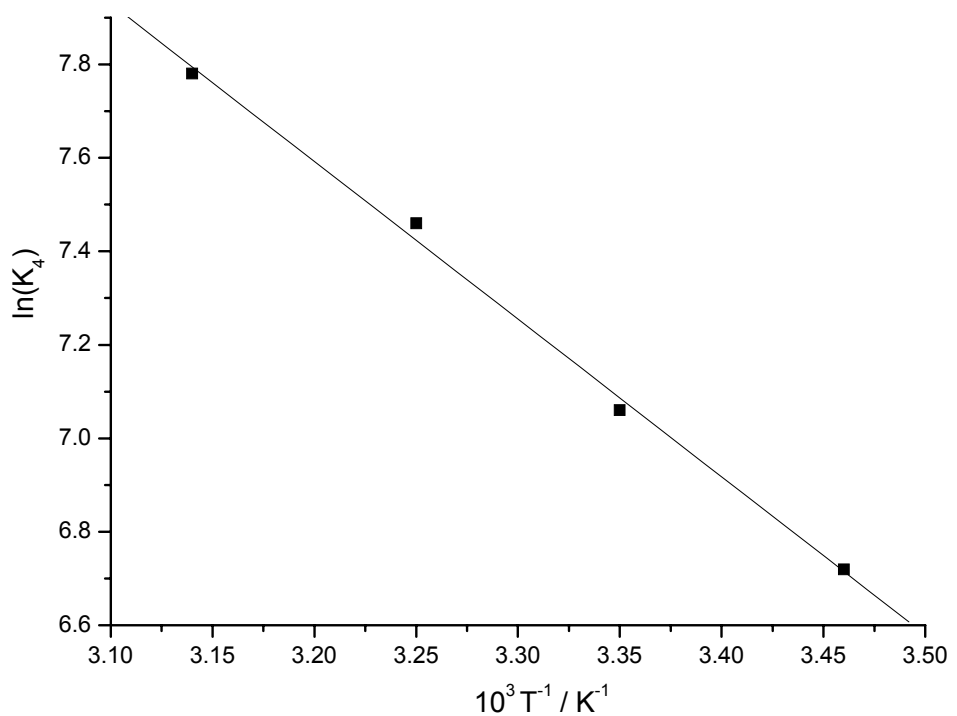


Figure S4

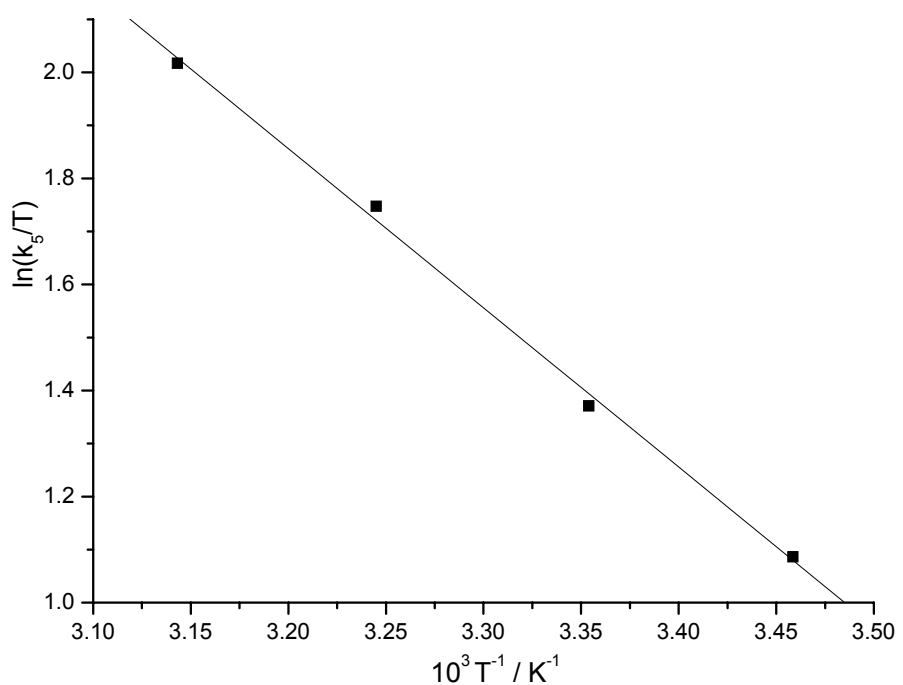


Figure S5

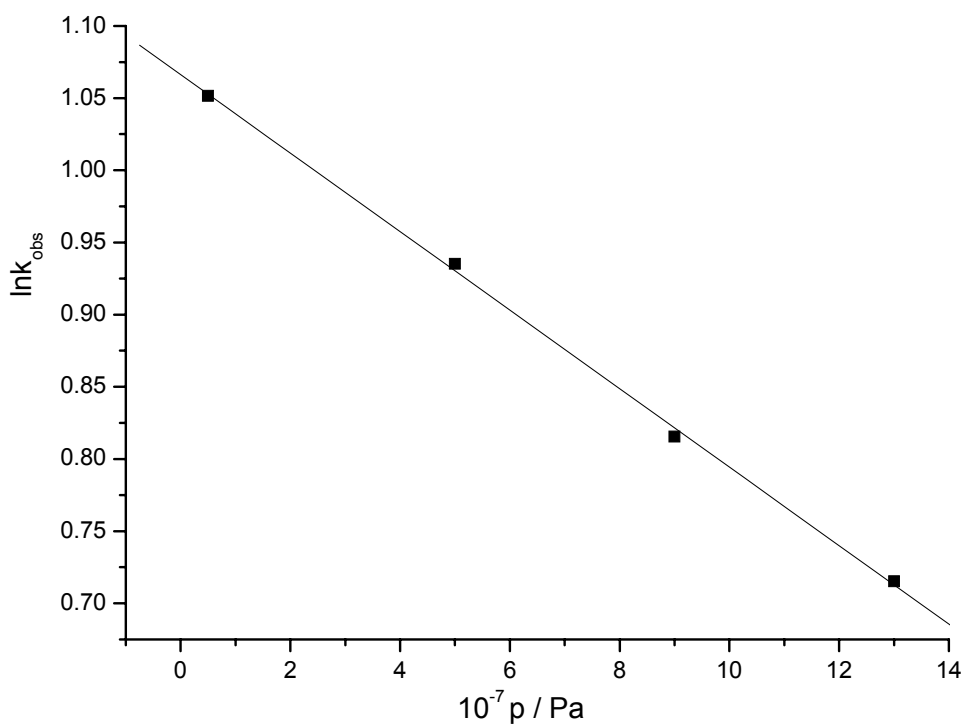


Figure S6

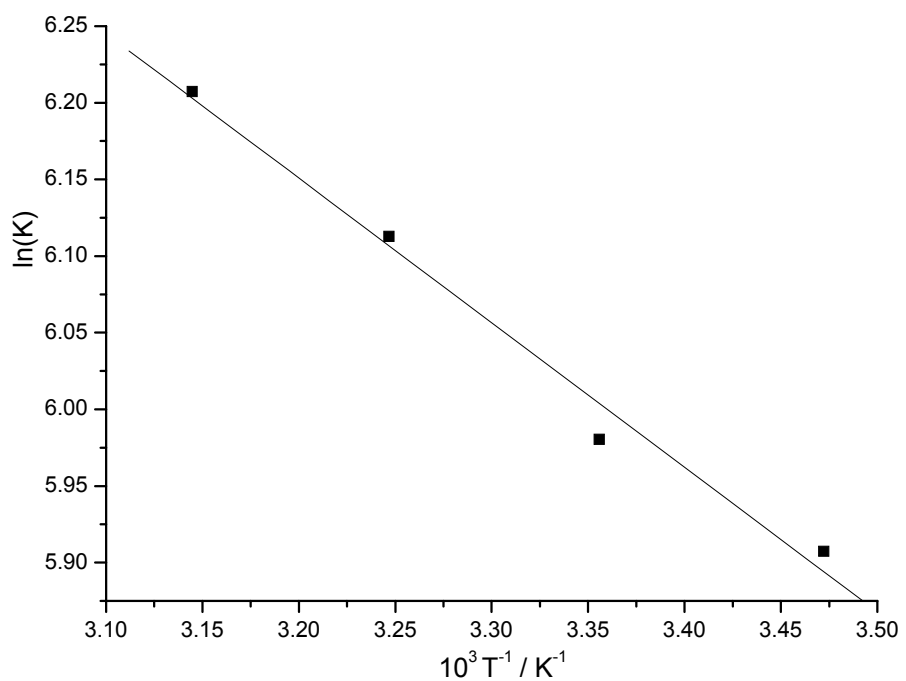


Figure S7

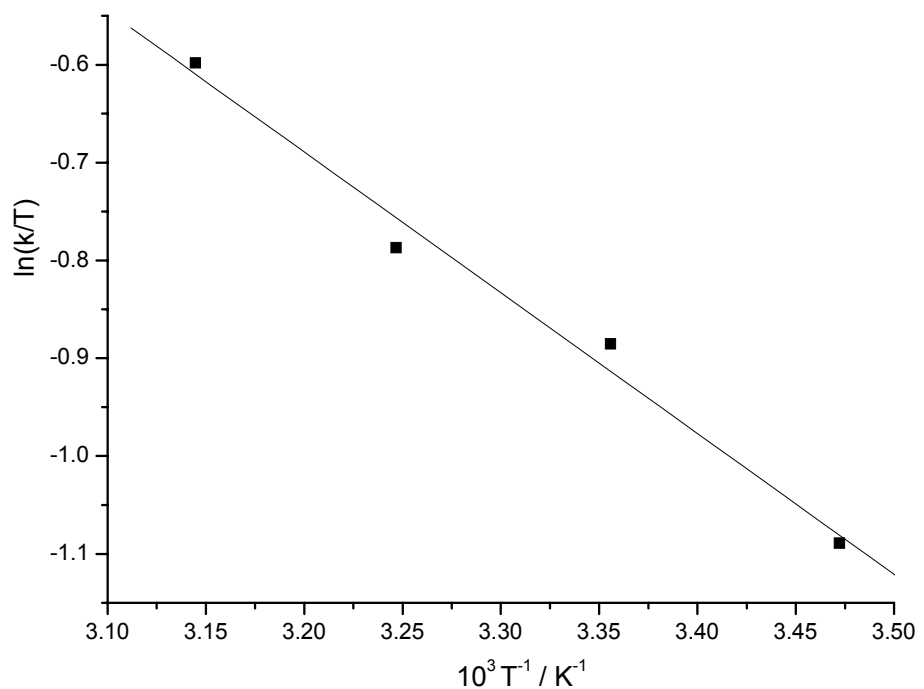


Figure S8

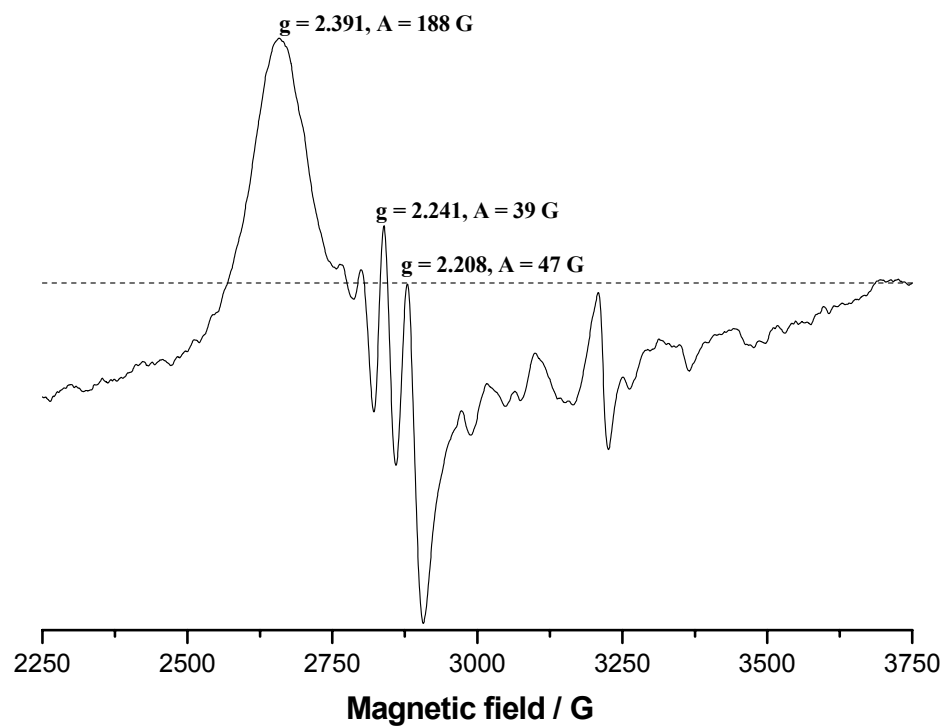


Figure S9

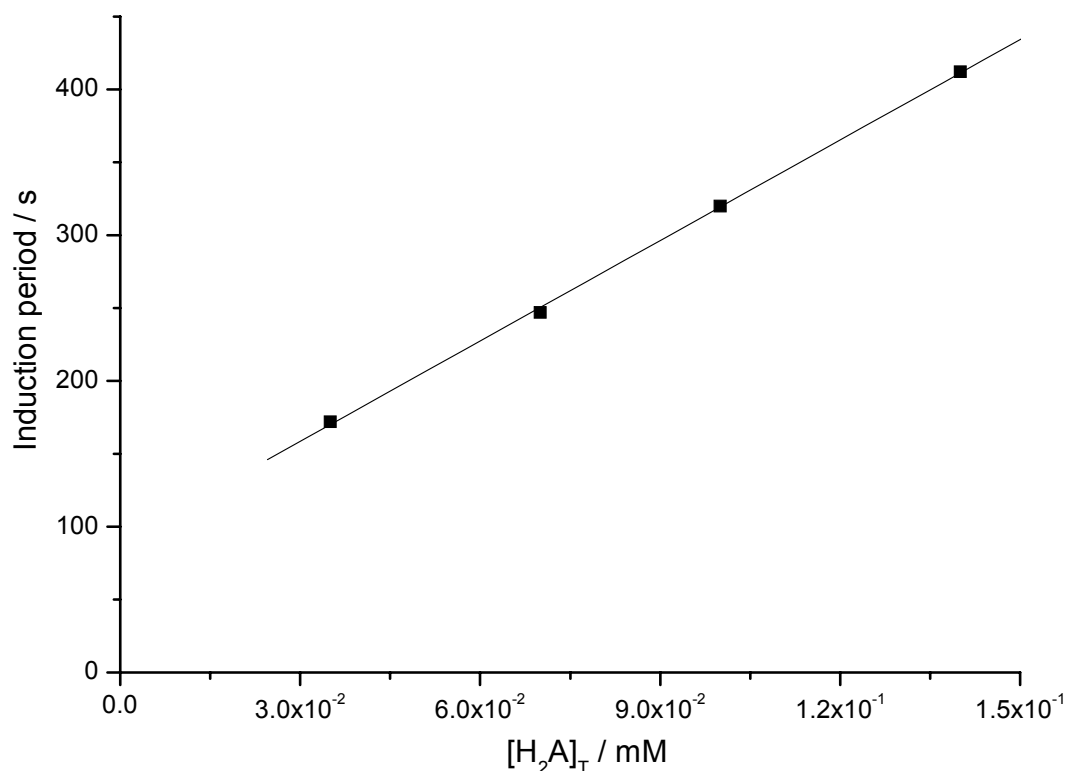


Figure S10

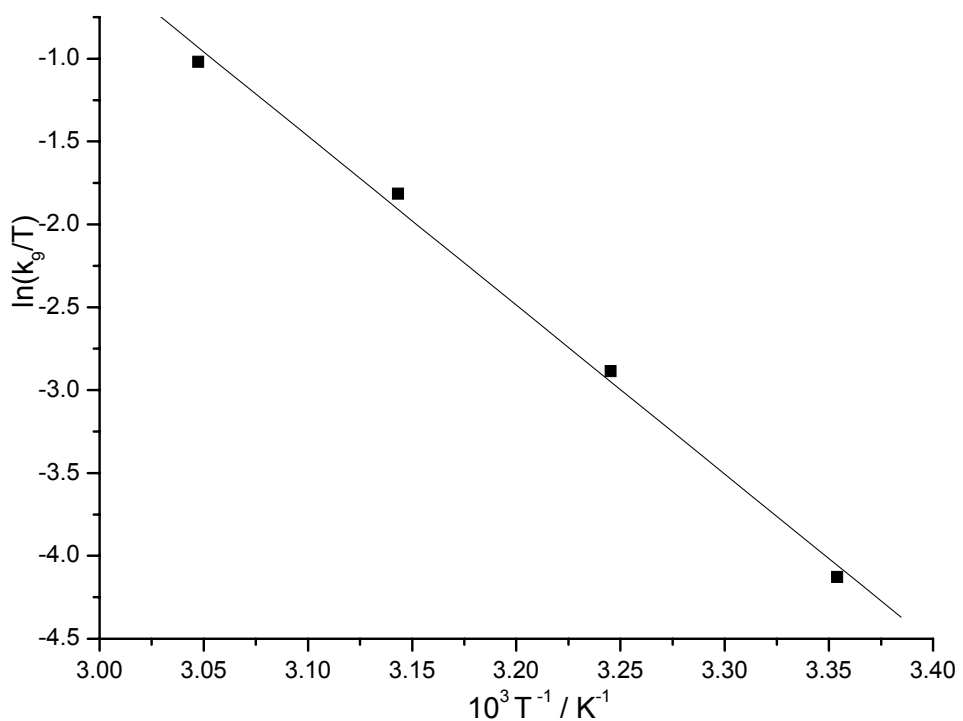


Figure S11

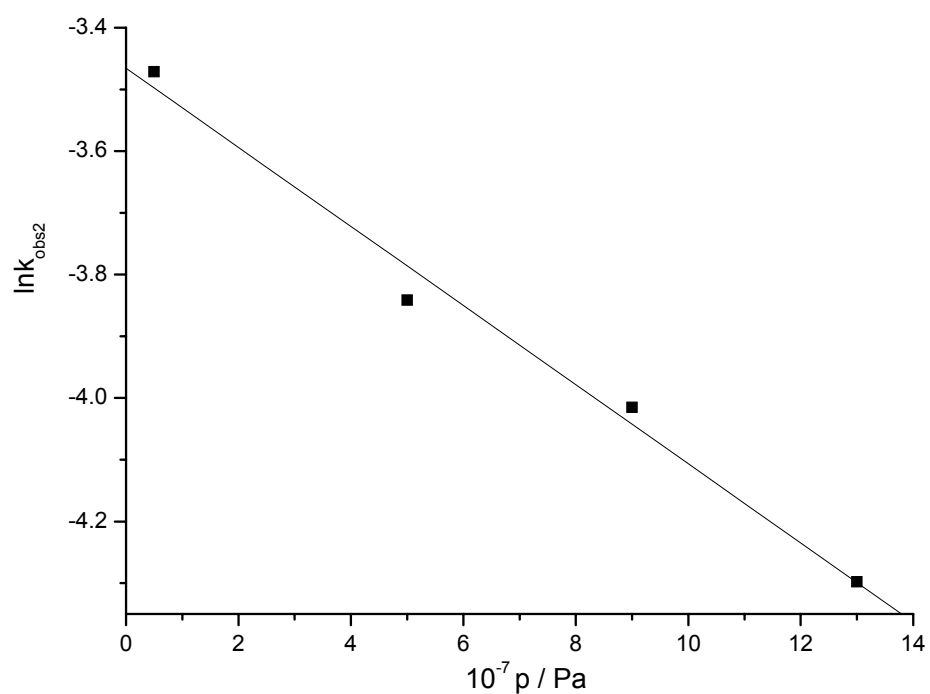


Figure S12

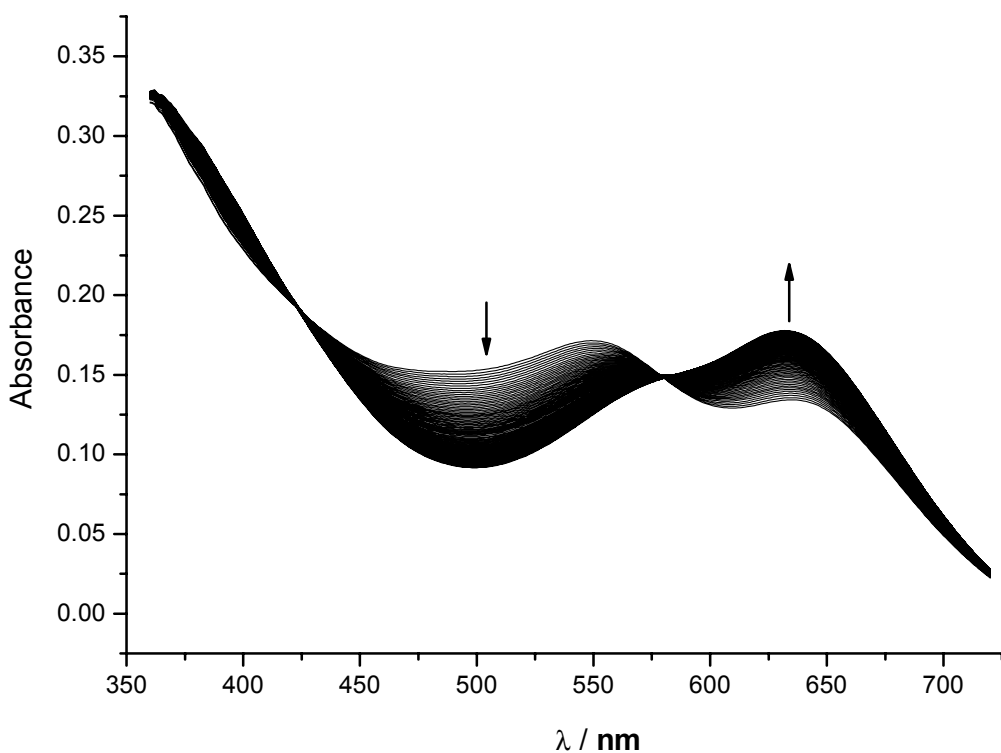


Figure S13

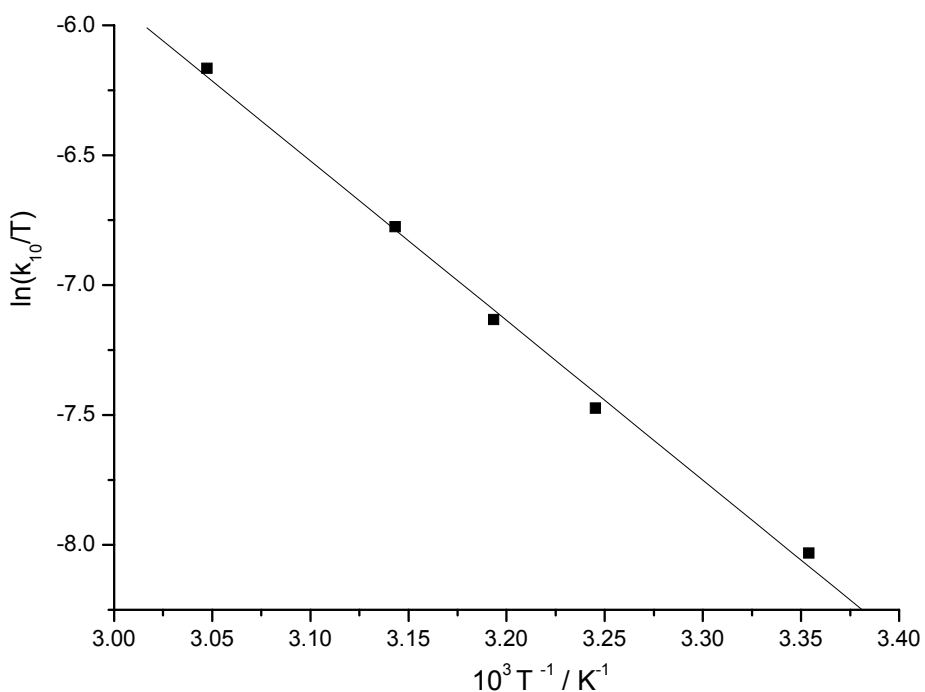


Figure S14

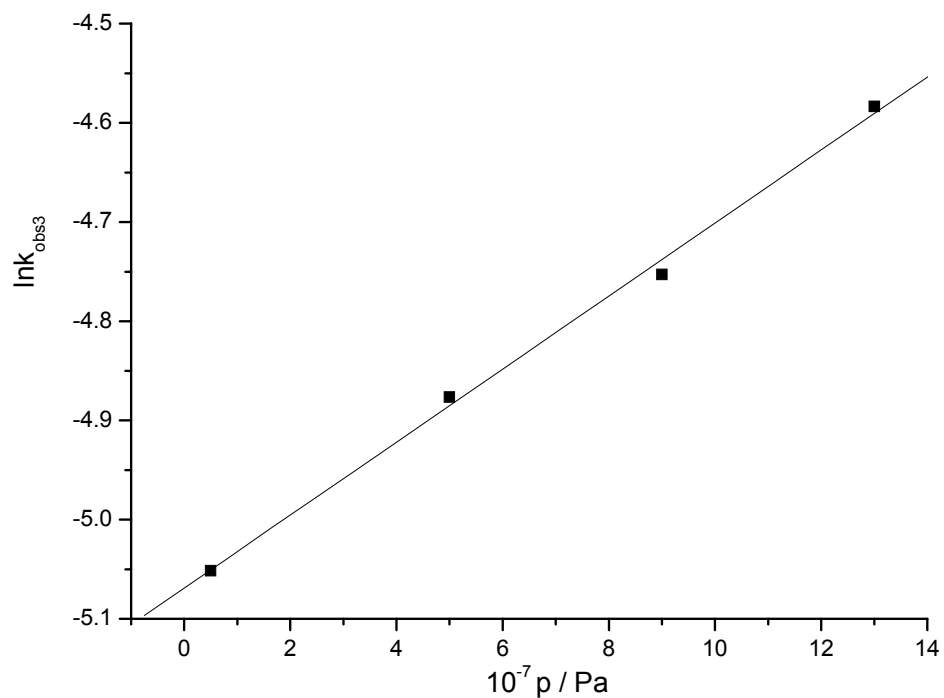


Figure S15

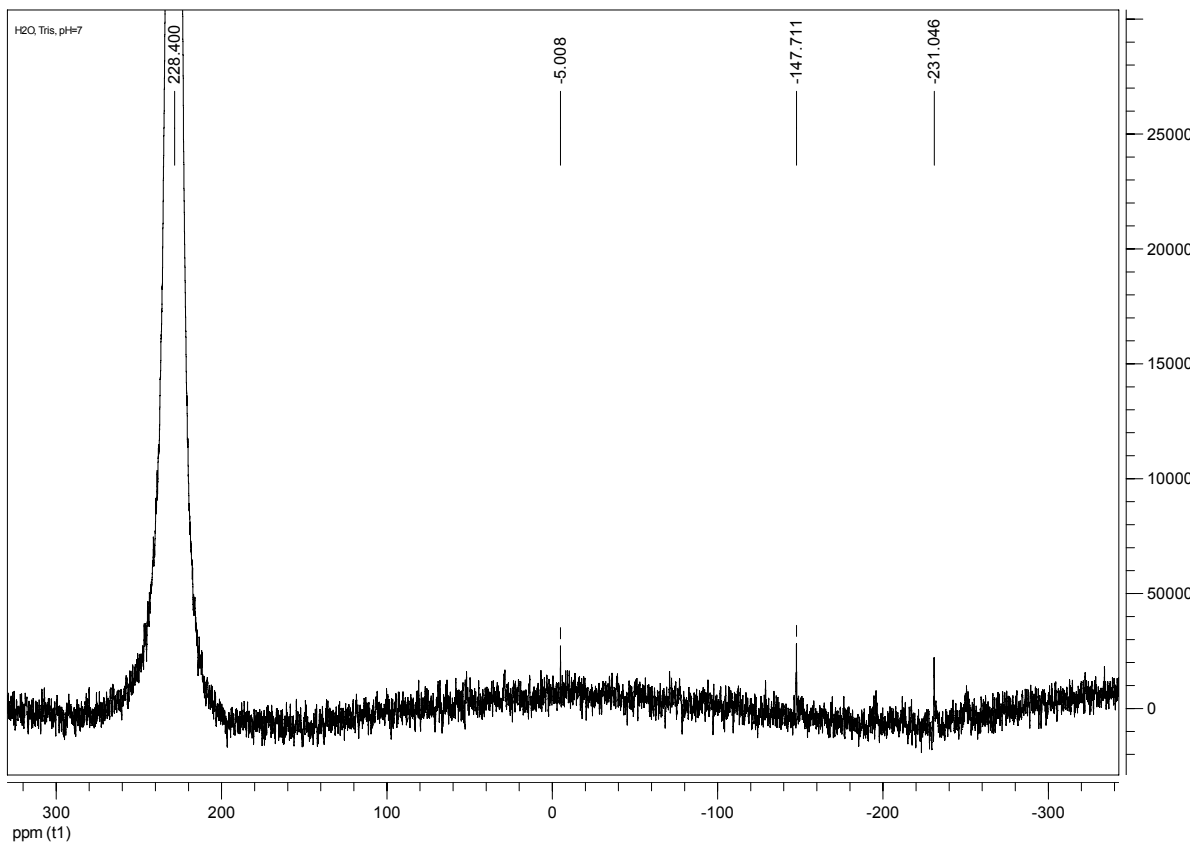


Figure S16